

This is the accepted manuscript made available via CHORUS. The article has been published as:

Ni-(In,Ga)As Alloy Formation Investigated by Hard-X-Ray Photoelectron Spectroscopy and X-Ray Absorption Spectroscopy

Lee A. Walsh, Greg Hughes, Conan Weiland, Joseph C. Woicik, Rinus T. P. Lee, Wei-Yip Loh, Pat Lysaght, and Chris Hobbs

Phys. Rev. Applied **2**, 064010 — Published 30 December 2014

DOI: [10.1103/PhysRevApplied.2.064010](https://doi.org/10.1103/PhysRevApplied.2.064010)

Investigation of Ni-InGaAs alloy formation by hard x-ray photoelectron spectroscopy and x-ray absorption spectroscopy

Lee A. Walsh* and Greg Hughes

Dept. of Physical Sciences, Dublin City University, Glasnevin, Dublin 9, Ireland

Conan Weiland and Joseph C. Woicik

National Institute of Standards and Technology, Gaithersburg, Maryland 20899, USA

Rinus T.P. Lee, Wei-Yip Loh, Pat Lysaght, and Chris Hobbs

SEMATECH, 257 Fuller Road, Suite 2200, Albany, New York 12203, USA

The electrical, chemical, and structural interactions between Ni films and InGaAs for source/drain applications in transistor structures have been investigated. It was found that for thick (>10 nm) Ni films a steady decrease in sheet resistance occurs with increasing anneal temperatures, however, this trend reverses at 450°C for 5 nm thick Ni layers, primarily due to the agglomeration/phase separation of the Ni-InGaAs layer. A combined hard x-ray photoelectron spectroscopy (HAXPES) and x-ray absorption spectroscopy (XAS) analysis of the chemical structure of the Ni-InGaAs alloy system shows: (1) that Ni readily interacts with InGaAs upon deposition at room temperature resulting in significant inter-diffusion and the formation of NiIn, NiGa, and NiAs alloys, and (2) the steady diffusion of Ga through the Ni layer with annealing, resulting in the formation of a Ga_2O_3 film at the surface. The need for the combined application of HAXPES and XAS measurements to fully determine chemical speciation and sample structure is highlighted and this approach is used to develop a structural and chemical compositional model of the Ni-InGaAs system as it evolves over a thermal annealing range of 250 to 500°C .

I. INTRODUCTION

The III-V materials, such as GaAs and InGaAs, show promise as a Si replacement as the channel material in n-MOSFETs due to their higher injection velocities and electron mobilities. Research has recently focused on InGaAs due to promising improvements in the InGaAs/high- κ interface [1–5], however, the issue of source/drain (S/D) contacts in InGaAs based MOSFETs remains. A possible solution is to find a self-aligned silicide-like material (salicide), to act as the S/D contacts [6]. The optimum material would ideally display an abrupt ordered interface with InGaAs, low sheet resistance (R_{sh}), as well as achieving the thermal stability to withstand the temperatures involved in current MOSFET fabrication processes. The search for this material has recently focussed on the Ni-InGaAs system, due to its promisingly low R_{sh} , and its apparent sharp interface with InGaAs [6–8]. In addition, investigations have been performed on the ability to incorporate this material system into standard device processing procedures [7, 9]. There is a large body of work detailing the chemical interaction between Ni and GaAs, and Ni and InP, yet there is significantly less published data on the Ni-InGaAs system which is known to form a mixed metallic alloy phase [10–13]. Previous studies have shown a trend of decreasing R_{sh} with increasing post deposition anneals, although there is a reversal in this trend between 450 to 500°C [7, 14]. While it has been suggested that this change

could be attributed to the thermal desorption of the III-V elements at this anneal temperature, more detailed work is needed to understand this behaviour. The aim of this study is to address this issue by exploring the details of the chemical bond formation resulting both from the initial Ni deposition as well as the structural changes which occur after a range of thermal anneals up to 500°C .

X-ray photoelectron spectroscopy (XPS) is a widely used technique for the identification of chemical changes at metal/semiconductor interfaces, and can readily detect the oxidation state of the chemical species present. Additionally, XPS can be used to quantitatively determine non-destructive depth-dependent composition due to the well characterized photoelectron attenuation lengths [15]. Hard XPS (HAXPES) using x-ray photons of higher energy than conventional XPS can increase the effective sampling depth of the photoemission measurement to greater than 20 nm into the material [1, 16, 17]. Chemical speciation in XPS, however, is complicated by the dependence of peak energies and shapes on electrostatic interactions such as interfacial dipoles or fixed charges; that is, chemical differences cannot always be judged by apparent binding energy (BE) shifts alone. X-ray absorption spectroscopy (XAS) measures the absorption edges of the individual elements in a material to deduce information about their local bonding environment [18]. Unlike XPS, fluorescence yield hard x-ray XAS is unaffected by sample charging, reducing the uncertainty in chemical speciation. In the analysis of XAS measurements the spectra can be compared with those of reference materials thereby assisting in the identification of the chemical species present. This paper demonstrates

* lee.walsh36@mail.dcu.ie

the advantage in combining these two techniques, to obtain a clear chemical and structural model of a complex material system.

In this study, nickel films of different thicknesses were sputter deposited on undoped InGaAs substrates and thermally annealed at a range of temperatures between 250 and 500 °C in 50 °C steps. These samples were then investigated using sheet resistance, XAS, scanning electron microscopy (SEM), transmission electron microscopy (TEM) and HAXPES measurements in order to obtain information on the electrical resistivity, the chemical composition and the physical structure of the Ni/InGaAs interfacial region. Grazing incidence XAS measurements were used to identify the chemical phases present in the Ni/InGaAs interfacial region and compared to more bulk sensitive measurements.

II. EXPERIMENTAL

The undoped InGaAs samples consisted of 30 nm thick $\text{In}_{0.53}\text{Ga}_{0.47}\text{As}$ layers grown by molecular beam epitaxy (MBE) on InAlAs epi-ready layers on InP substrates. The samples were cleaned for 60 seconds in dilute hydrofluoric acid prior to being loaded into the metal deposition chamber. The samples for electrical and TEM measurements were produced with 5, 15, and 25 nm thick sputter-deposited Ni layers, and separate samples were prepared by annealing in 50 °C steps between 250 and 500 °C for 60 seconds. For HAXPES analysis one sample was left bare to act as a clean InGaAs reference, while all other samples had 5 nm of Ni sputter-deposited. One of these Ni capped samples was left unannealed, while the remaining samples were annealed in-situ in the deposition chamber in 50 °C steps between 250 and 500 °C. In order to study the changes in the relative intensities of the peaks as a function of thermal annealing, which can assist in determining the extent of inter-diffusion and hence the location of the chemical species, an internal reference peak which remains at constant intensity is necessary. This was achieved by capping all of the HAXPES samples with a sputter deposited 3 nm SiN capping layer in a separate chamber, after the Ni deposition and anneal, to act both as a barrier to post processing oxidation and as an internal reference. As such the Si 1s peak was acquired at the same time as each core level, with a constant ratio between the number of scans of the Si 1s and the relevant core level of 1:4. This was subsequently used to correct for any photon energy drift during the measurements, and to normalise the intensity of the core level spectra across all samples. Using the Si 1s reference spectra for each core level, the change in peak intensity of a given chemical species throughout the anneal study can be determined, and thus the diffusion behaviour of the different elements can be investigated [19]. An equivalent sample set, was prepared using identical conditions for the XAS measurements. However, the SiN layer was not present, as a reference layer is not required in XAS.

Electrical sheet resistance (R_{sh}) measurements were performed on the annealed samples using a four-point probe apparatus. The samples for TEM analysis were prepared using a dual beam FIB equipped with an in-situ nano-manipulator. The samples were first protected by applying layers of electron beam deposited C and Pt, and then a second layer of Pt was deposited using the ion beam. The samples were thinned to electron transparency using 30 kV and 7 kV Ga ion beams followed by a 2 kV clean up step. The samples were imaged using a STEM apparatus operated at 300 kV and the images were recorded using a beam convergence angle of 8.1 mRad. TEM images were filtered to produce zero-loss images with a 10 eV energy window.

HAXPES measurements were carried out on the National Institute of Standards and Technology (NIST) beamline (X24A) at the National Synchrotron Light Source (NSLS) at Brookhaven National Laboratory (BNL). A double Si (111) crystal monochromator allowed for photon energy selection in the range of 2.1 to 5.0 keV. An electron energy analyser was operated at a pass energy of 200 eV giving an overall experimental broadening of 0.29 eV at the chosen photon energy of 2200 eV, 0.43 eV at 3000 eV, and 0.52 eV at 4050 eV. The total sampling depth of the HAXPES measurement using a photon energy of 2200 eV is estimated to be 13 nm [20] which ensures the detection of photoemitted electrons from the 3 nm SiN and 5 nm Ni layers, as well as approximately 6 nm into the InGaAs, which is obtained from the inelastic mean free path of the As $2p_{3/2}$, Ga $2p_{3/2}$, and In $3d_{5/2}$ photoemitted electrons at this photon energy [21]. The sampling depth is estimated to be 18 nm and 21 nm for 3000 eV and 4050 eV, respectively. The XPS core level spectra were curve fitted using Voigt profiles composed of Gaussian and Lorentzian line shapes with a Shirley-type background [22].

Fluorescence yield hard x-ray XAS measurements were performed on the As, Ga, and Ni K-edges at room temperature using the NIST beamline (X23A2) at the NSLS. A double Si (311) crystal monochromator allowed for photon energy selection in the range of 4.9 to 30 keV. XAS measurements were performed with the angle between the incident beam and sample surface at the critical angle (approximately 0.15°) to produce surface sensitive data and at both 0.5° (Ga and As K-edges) and 1.2° (Ni K-edge) to sample either the entire Ni film and/or a more bulk sensitive InGaAs signal. The grazing incidence angle chosen was at a critical angle of 0.15° where the x-ray photon penetration depth into the sample is 2.5 to 5 nm. Below the critical angle total external reflection occurs. The XAS signal is entirely bulk sensitive at an incidence angle of 1° [23], where an incidence angle of 90° is normal to the sample surface.

III. RESULTS AND DISCUSSION

In order for Ni-InGaAs to be incorporated into the processing of III-V MOSFETs, it is critical to know the effect of both anneal temperature and initial Ni thickness (t_{Ni}) on the electrical resistance. The sheet resistance of the Ni-InGaAs samples over a range of annealing temperatures was determined by four point probe measurements. Figures 1 (a) and (b), show the plots of R_{sh} for a 5 nm and a 15 nm thick Ni layer, respectively, annealed in 50 °C steps between 250 and 500 °C. A consistent drop in R_{sh} with increasing anneal temperature up to 400 °C is observed for the 5 nm deposited layer, with the trend reversing for higher temperatures. This reversal is not observed for the 15 nm film which is attributed to the decreasing influence of Ni-InGaAs interface effects as the thickness of the deposited layer is increased. The even lower value of sheet resistance for the 25 nm Ni film following a 400 °C anneal evident from Figure 1 (c) confirms this trend in agreement with previous studies of the Ni-InGaAs system [7–9].

Cross-sectional TEM measurements and top down SEM images of the 5 nm deposited samples following the 250, 400, and 500 °C anneals were taken in order to determine the morphological changes in the Ni-InGaAs layer occurring over the course of the anneal study, and in particular if any significant difference could be observed following the 500 °C anneal. In the TEM image in Figure 2 (a) for the 250 °C anneal sample, a uniform thickness Ni-InGaAs layer can be clearly distinguished. When the anneal temperature is increased to 400 °C the Ni-InGaAs layer thickness increases suggesting increased inter-diffusion. After the 500 °C anneal, there is evidence of significant disruption of the ordered layer structure apparent at lower temperatures and agglomeration/phase separation is seen in the Ni-InGaAs layer. This effect is also seen in SEM images, displayed in Figure 2, which show a substantial increase in surface roughness and evidence of islanding in the 500 °C sample as compared to 250 °C and 400 °C samples. This is a possible reason for the increase in sheet resistivity seen in Figure 1 (a) following a 500 °C anneal, as the sample surface is no longer fully covered by a uniform Ni-InGaAs layer due to the disruption of the layered structure.

In order to further understand the decrease and subsequent increase in R_{sh} with increasing anneal temperature for the 5 nm deposited Ni film, it is necessary to determine the changes in the sample chemistry which occur in the Ni-InGaAs interfacial region probed by XAS and HAXPES measurements. The normalised HAXPES spectra of the In $3d_{5/2}$, As $2p_{3/2}$, and Ga $2p_{3/2}$ core levels for the SiN capped InGaAs reference sample with no nickel layer are shown in Figure 3. The spectra are fitted according to the parameters specified by *Brennan et al* [24], who compiled a wide variety of reported oxide positions for the InGaAs core level peaks. It is clear from the presence of higher BE components in the individual elemental spectra that the InGaAs surface was partially

oxidised due to air exposure prior to SiN deposition. The corresponding As and Ga absorption K-edges from the XAS measurements of this sample for both surface and bulk sensitive modes, shown in Figure 3 (b), reflect the homogenous composition within the XAS sampling depth and match reference spectra of GaAs and InAs samples [25, 26]. The surface sensitive As K-edge spectra show evidence of oxidation, seen as an increase in the white line peak intensity (at 11868 eV) compared to the bulk sensitive spectra, which is consistent with As oxidising more readily than Ga at GaAs and InGaAs surfaces [27].

To understand the change in the chemical structure of the sample throughout the study, it is necessary to study both the chemical species present at each anneal stage and the location and relative concentration of these chemical species within the sample. As stated earlier the use of an internal reference peak, such as the Si $1s$ peak used here, allows the location of each chemical species to be determined. The Si $1s$ core level spectra acquired from the SiN capping layers on the bare InGaAs sample and the Ni-InGaAs sample as-deposited and following a 500 °C anneal, as shown in Figure 4, display a very similar profile, apart from an increase in the higher BE shoulder at +1.5 eV. The SiN surface would be expected to oxidise after removal from the deposition chamber, forming a thin layer of Si_2N_2O or SiO_2 [28], however, this would be expected to be similar for all samples. Therefore, the increased level of Si oxidation apparent for the samples with the Ni interlayer would suggest that this oxidation has occurred at the SiN/Ni interface which will be discussed later.

Figure 5 (a) shows the normalised (to the Si signal in the SiN capping layer) and curve fitted Ni $2p_{3/2}$ HAXPES spectra acquired at 2200 eV photon energy for the SiN-Ni-InGaAs samples as-deposited (20 °C) and after 300 °C and 400 °C anneals. The spectra are fitted with two peaks, the metal Ni peak at 0 eV, and a broad plasmon loss feature at +2.4 eV [29]. The metallic peak is fitted using an asymmetric Voigt function with Lorentzian values of 0.46 ± 0.05 eV, and Gaussian values of 0.55 ± 0.05 eV. The decrease in the intensity of the Ni $2p_{3/2}$ peak with successively higher anneals suggests either the diffusion of the Ni into the InGaAs, and/or the diffusion of the InGaAs substrate elements through the Ni. However, there is no obvious change in the lineshape of the Ni $2p_{3/2}$ throughout the annealing study which indicates that no strong chemical interaction between the Ni and InGaAs can be detected by HAXPES measurements of the Ni $2p$.

Figure 5 (b) shows the Fourier transformed Ni K-edge XAS spectrum of a reference polycrystalline metal Ni foil and the Ni-InGaAs sample prior to any anneal. It is clear that the deposited Ni is not in a metallic Ni chemical environment, suggesting that significant intermixing with the InGaAs has occurred upon deposition. The Ni K-edge spectra for the as-deposited layer shown in Figure 5 (c), acquired in both bulk and surface sensitive modes,

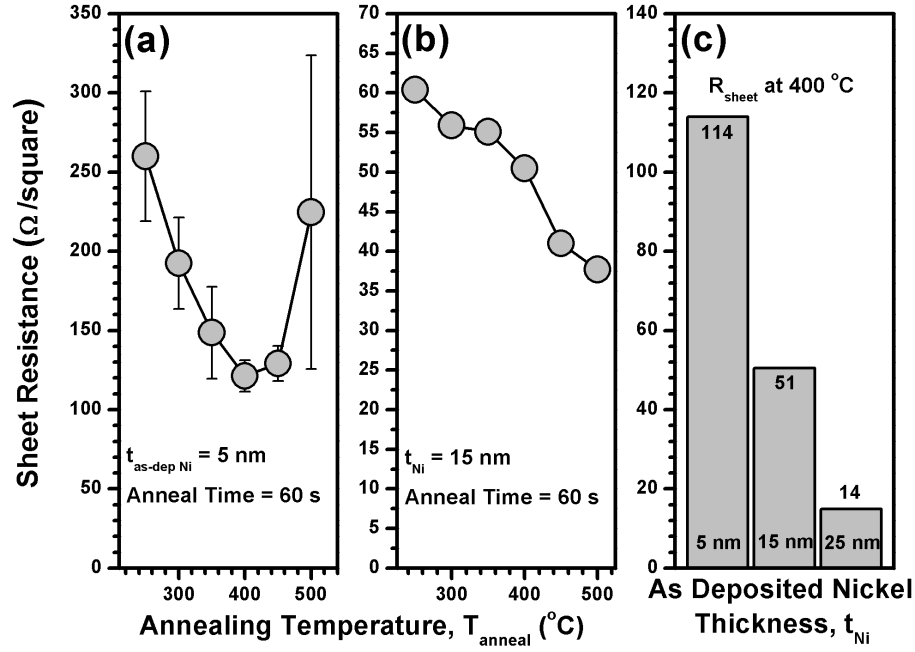


FIG. 1. Sheet resistance measurements (a) on 5 nm and (b) 15 nm thick Ni layers as a function of post deposition anneal temperature and (c) as a function of Ni thickness after a 400 $^{\circ}\text{C}$ anneal.

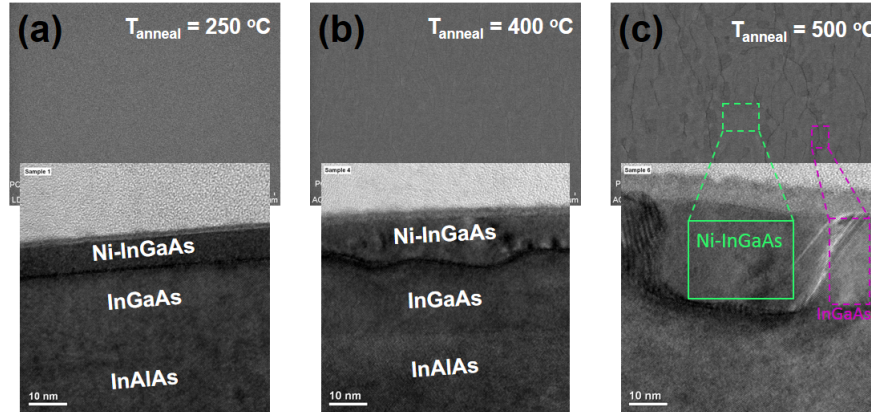


FIG. 2. SEM (top) and TEM (bottom) images of 5 nm Ni capped samples after (a) 250 $^{\circ}\text{C}$, (b) 400 $^{\circ}\text{C}$, and (c) 500 $^{\circ}\text{C}$ post deposition anneals showing the increasing thickness of the Ni-InGaAs following the 400 $^{\circ}\text{C}$ anneal and the agglomeration/phase separation which occurs following the 500 $^{\circ}\text{C}$ anneal.

match the XAS spectrum of NiGa [30]. While the two stepped structure (with step features at 8334 and 8342 eV) is weaker in the as-deposited film, possibly due to a mixed NiGa and metallic Ni phase in the reacted layer, this structure becomes more prominent in both the bulk and surface spectra after 250 $^{\circ}\text{C}$ anneal (not shown) indicating the continued formation of a NiGa phase. The NiGa formation also indicates that Ga atoms have diffused into the Ni layer at room temperature. Increasing the anneal temperature to 400 $^{\circ}\text{C}$, as seen in Figure 5 (c) results in the surface spectrum still resembling a NiGa alloy, but the bulk spectrum begins to show a change

consistent with a chemically mixed phase of NiGa and NiAs, or NiAs₂, as suggested by the appearance of peaks at 8344 eV and 8353 eV in the bulk sensitive spectra [31]. After a 500 $^{\circ}\text{C}$ anneal (not shown) the peaks at 8342 and 8352 eV in the bulk sensitive spectrum which are assigned to NiAs become more prominent, while the surface sensitive signal also displays the same NiAs features. Even for the highest anneal temperature, both surface and bulk sensitive spectra display a mix of NiGa and NiAs bonding configurations, once again confirming the diffusion of Ga through the Ni layer, and continued formation of NiAs. There is no evidence of Ni oxida-

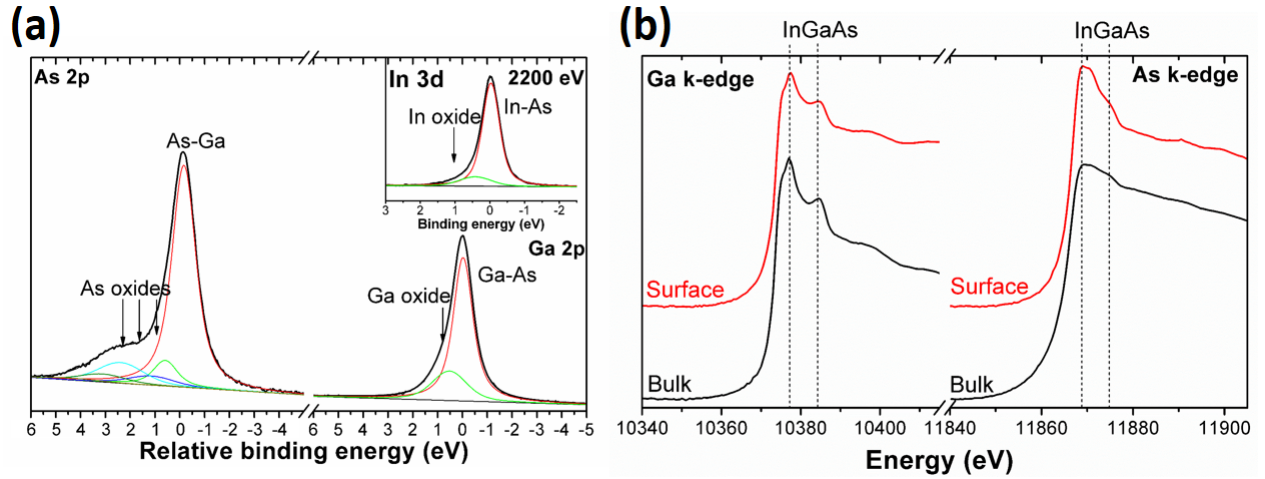


FIG. 3. (a) Normalised and fitted $\text{In } 3dd_{5/2}$, $\text{As } 2pd_{3/2}$, and $\text{Ga } 2pd_{3/2}$ HAXPES spectra acquired at a photon energy of 2200 eV for a SiN-InGaAs sample showing surface oxidation of the InGaAs layer. The spectra are plotted relative to the binding energy of the substrate InGaAs peaks, As-Ga for the $\text{As } 2pd_{3/2}$, Ga-As for the $\text{Ga } 2pd_{3/2}$ and In-As for the $\text{In } 3dd_{5/2}$. (b) XAS spectra of As and Ga K-edges showing the similarity in surface and bulk sensitive spectra of the InGaAs material consistent with a uniform chemical composition within the XAS sampling depth.

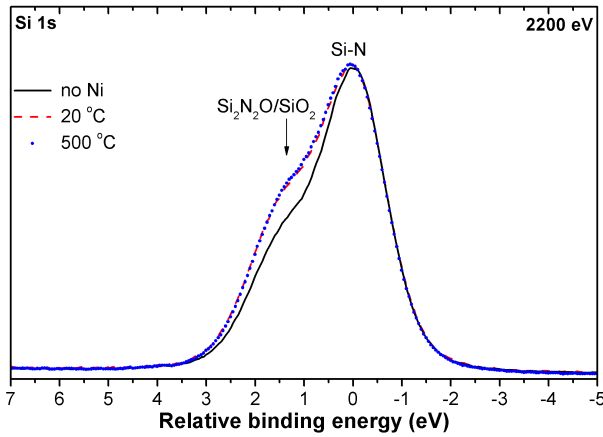


FIG. 4. Normalised $\text{Si } 1s$ spectra for the SiN capping layer with (20 °C) and without Ni and after 500 °C anneals. The spectra are plotted relative to the binding energy of the Si-N peak.

tion in any of the samples. It is important to note that from the HAXPES measurements no chemical change in the Ni spectra is detected, while the XAS identifies a large Ni-InGaAs interaction resulting in a variety of Ni compounds, which evolve as the anneal temperature increases. This indicates that the chemical reaction between the Ni and InGaAs initiates upon Ni deposition and the only change following anneal is the continued reaction and interdiffusion between the Ni and InGaAs. As the XAS identifies the bonds present in the surface and bulk of the reacted layer, a difference is seen following anneal due to the diffusion of Ga through the sample, leading to the NiGa being located closer to the sample surface than the NiAs.

Figure 6 (a) shows the HAXPES spectra for the normalised and curve fitted $\text{Ga } 2p_{3/2}$ core level acquired at 2200 eV photon energy for the SiN-InGaAs sample and the SiN-Ni-InGaAs sample, as-deposited (20 °C) and after a 400 °C anneal. The spectrum from the SiN-InGaAs sample is fitted with two peaks, one representing the Ga-As peak present in the InGaAs bulk, and one which is attributed to Ga_2O due to surface oxidation. The spectrum of the as-deposited SiN-Ni-InGaAs sample shows the growth of a broad peak at +1 eV BE, consistent with an oxidised Ga state, although it is difficult to be definitive as to the exact stoichiometry of the oxide as the attenuation of the substrate Ga-As peak removes the reference by which the oxidation state is normally identified [32]. In addition to the oxide growth, the lower BE peak at -0.5 eV is attributed to a Ga-Ni bonding interaction at the surface based on the respective electronegativities of both Ga (1.81) and Ni (1.91) [33]. The reaction between Ga and Ni has been studied previously on GaAs and the observed strong interaction between Ni and Ga [12] was attributed to the large enthalpy of formation for NiGa [34]. As the anneal temperature increases to 400 °C a large growth in the Ga oxide peak, at +1 eV, is seen, and a decrease in the Ga-Ni intensity. This assignment is consistent with inter-diffusion between the InGaAs and Ni layer as has been previously reported for the interaction between Ni and Ga containing semiconductors [34, 35]. The subsequent oxidation of the up-diffused Ga, prior to SiN deposition, results in the formation of a surface oxidised overlayer which acts to suppress the Ga-Ni signal. The $\text{Ga } 2p_{3/2}$ spectra following the 500 °C anneal (not shown) is similarly dominated by the Ga oxide peak, indicating the formation of a thick Ga oxide layer prior to the deposition of the SiN cap.

The bulk sensitive Ga K-edge spectra shown in Fig-

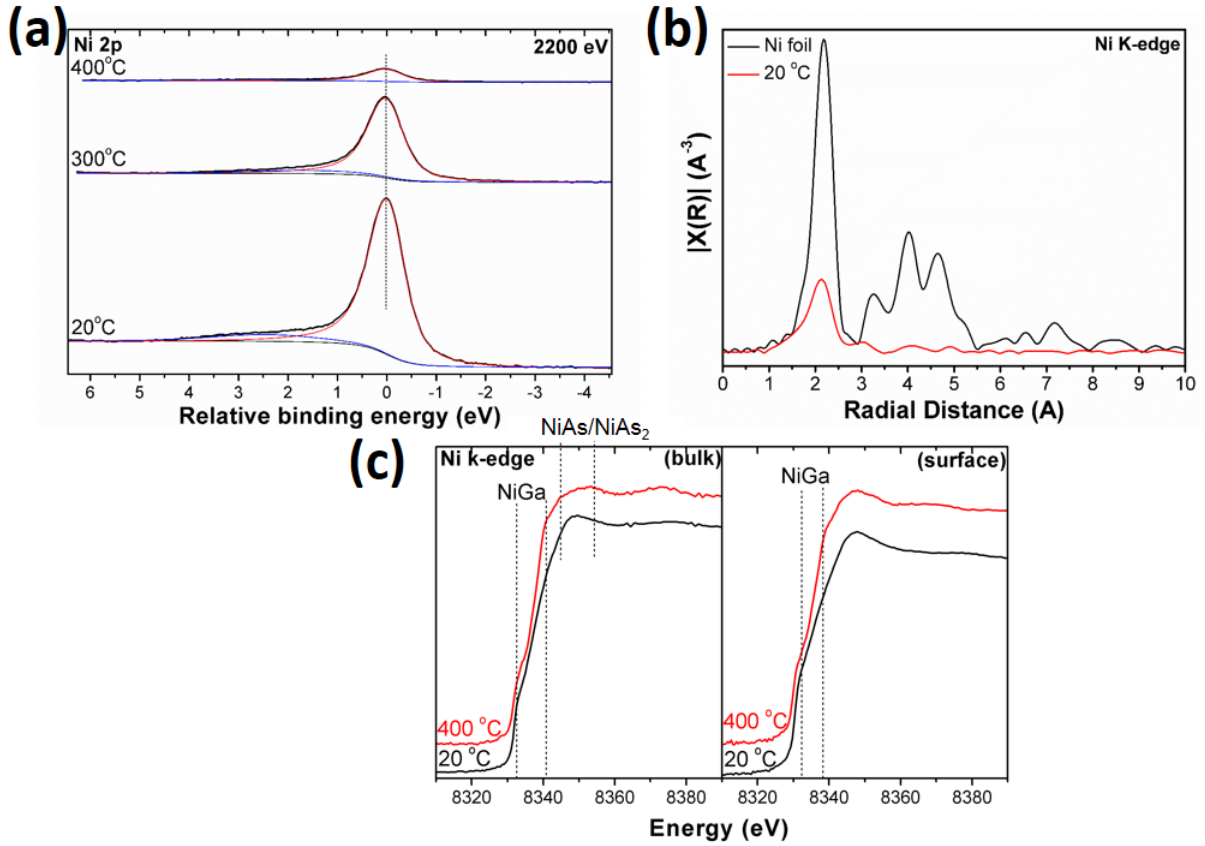


FIG. 5. (a) Normalised and fitted Ni $2p_{3/2}$ HAXPES spectra for SiN-Ni-InGaAs samples as-deposited (20 °C) and after 300 °C and 400 °C anneals. The spectra are plotted relative to the binding energy of the main Ni peak. (b) Fourier transformed XAS spectra of the Ni K-edge, for a reference Ni foil and the Ni signal from the as-deposited (20 °C) Ni-InGaAs sample and (c) XAS spectra from the as-deposited (20 °C) Ni-InGaAs sample, after 400 °C anneal.

ure 6 (b) for InGaAs samples with and without Ni are indicative of the gallium atoms being in either a GaAs or InGaAs bonding environment with the characteristic two peak structure at 10378 and 10384 eV [25]. However, with Ni deposition, the surface sensitive spectrum shows significant changes, and the appearance of a broad feature at 10380 eV, which could suggest the presence of NiGa or oxidised Ga at the surface of the Ni-InGaAs film [36, 37]. This additional feature in the spectrum is less evident in the bulk sensitive spectra shown in Figure 6 (b) again suggesting that this species is localised at the top of the Ni layer. Figure 6 also shows the spectra for a Ni-InGaAs sample following a 400 °C anneal where the appearance of a structure (double peak feature at 10379 and 10382 eV) matching Ga_2O_3 is seen, in agreement with previous studies [36–38]. Direct evidence for the formation of NiGa bonds cannot be determined from these spectra due to the fact that the primary feature of NiGa appears at 10378 eV [30], and thus would be difficult to distinguish from the Ga_2O_3 signal, although NiGa was previously detected in the Ni K-edge spectra. These results suggest that upon Ni deposition some Ga atoms diffuse through the Ni layer to the surface where they oxidise, which is assumed to have occurred when

the Ni-InGaAs samples were removed from the vacuum system. The 500 °C spectra (not shown) display very similar results to the 400 °C spectra. The Ga K-edge data is thus consistent with the picture provided by the Ni K-edge analysis.

The complementary chemical information derived from the HAXPES and XAS spectra is therefore particularly beneficial in the analysis of the Ga $2p_{3/2}$. In relation to the Ga $2p_{3/2}$ peak profile after Ni deposition the only evidence in the HAXPES spectra that this peak represents a different chemical state of the Ga is the large increase in the FWHM (1.38 eV in the oxide, as opposed to 0.78 eV in the Ga-As). The XAS spectra for the same sample acquired in a surface sensitive mode identifies the Ga signal to be in an oxidized state which is further confirmed by the HAXPES and XAS spectra following the 400 °C anneal, where the Ga oxide is identified as Ga_2O_3 . It is likely that oxidised Ga seen in the 20 °C spectra is composed of a number of suboxide states, and following anneal at 400 °C the greater concentration of Ga at the Ni-InGaAs surface forms Ga_2O_3 , which is the most stable of the Ga oxides [39].

The formation of Ga_2O_3 at the surface of the Ni-InGaAs reacted layer can be used to explain the changes

in SiN oxidation seen in Figure 4. The increase in the SiN-O signal in the as-deposited SiN-Ni-InGaAs sample is likely due to oxygen gettering by the SiN layer from the Ga_2O_3 at the SiN/Ni-InGaAs interface. The Gibbs free energies of SiN oxidation products, either SiO_2 ($G = -802$ kJ/mole) or $\text{Si}_2\text{N}_2\text{O}$ ($G = -1063$ kJ/mole) [28, 40], compared to Ga_2O_3 ($G = -998.3$ kJ/mole) [41] suggest that $\text{Si}_2\text{N}_2\text{O}$ could form at the SiN/Ni-InGaAs interface. The fact that there is no change in the extent of oxidation after a 500 °C anneal, where the Ga_2O_3 thickness is known to increase, indicates that this gettering behaviour is self-limiting.

Figure 7 displays the normalised and curve fitted In $3d_{5/2}$ spectra acquired at 2200 eV for the SiN-InGaAs sample and the SiN-Ni-InGaAs sample as-deposited (20 °C) and after a 400 °C anneal. For the reference SiN-InGaAs sample, the presence of a higher BE component shifted by +0.46 eV BE with respect to the In-As peak is indicative of an oxidised surface. A substantial change occurs upon deposition of the Ni layer resulting in the appearance of a very broad spectral feature which can be curve fitted with four component peaks. The two peaks on the lower BE side of the bulk In-As peak, are attributed to In-In bonds, at -1 eV and In-Ni bonds at -0.6 eV, consistent with the electronegativity values of In (1.78) and Ni [33]. Previous studies on the interaction of a deposited Ni layer with the InP surface, have reported the dissociation of the InP with the appearance of In-In bonds [10–12]. The In-Ni peak at -0.3 eV continues to grow as the anneal temperature increases. The strong increase in intensity of the In-Ni peak over the anneal range is attributed to the diffusion of In into the Ni layer, forming more In-Ni bonds in the layer below the Ga_2O_3 , while both the In-In and In-As signals are suppressed with increasing anneal temperature as both bonds are localised at the InGaAs interface.

XAS spectra of the In K-edge were recorded, however, due to the high energy (27000 eV) the peak was very broad making it hard to obtain information on the In bonding environment. The interpretation of the Ni K-edge spectra previously discussed suggests that any Ni-In formed is at a lower concentration than both NiAs and NiGa, as both of these alloys dominate the Ni edge spectra at different temperatures. However, due to the lack of XAS data, specific In chemical assignments are necessarily more speculative.

Figure 8 (a) shows the normalised and peak fitted As $2p_{3/2}$ spectra for the SiN-InGaAs sample and the SiN-Ni-InGaAs sample as-deposited and after 400 °C anneal. For the SiN-InGaAs sample, the As $2p_{3/2}$ profile has a higher BE component consistent with an oxidised surface. Although the overall line-shape does not significantly change in the as-deposited SiN-Ni-InGaAs sample, the substantial shift of +0.9 eV BE relative to the As-Ga peak, indicates a possible change in chemical state of the As located at the surface of the InGaAs, consistent with the formation of NiAs as also seen in the Ni K-edge data. Throughout the anneal study, the As chemical bonding

environments do not change, however, there is a significant reduction in the intensities of the overall As $2p_{3/2}$ peak as the anneal temperature is increased. As in the case for the Ni $2p_{3/2}$ peak in Figure 5, this is primarily attributed to the formation of the Ga_2O_3 layer above the InGaAs interface. Additionally, the substantial reduction in the intensity of the total As profile as a function of thermal anneal indicates that the As remains primarily localised at the InGaAs surface throughout the study. As K-edge spectra were acquired to confirm the sample composition profile, as shown in Figure 8 (b). The spectra of bare InGaAs are characteristic of a clean InGaAs, or a GaAs As K-edge spectrum, with a double peak structure at 11870 and 11875 eV [25] and the bulk spectra of the Ni-InGaAs sample show no change with anneal. The surface sensitive spectra do show a change indicative of a chemical interaction at the InGaAs surface, however, it has not been possible to identify the precise chemical species present, as the layer may consist of a number of As species, such as As-As, AsNi, and AsO_x . Upon annealing at 400 °C, there is a significant change in the surface sensitive spectra with a strong peak emerging at 11868 eV corresponding to NiAs or NiAs₂ phases [31, 42], while the bulk sensitive signal shows no change. Following the 500 °C anneal (not shown), the surface sensitive spectrum becomes less well defined, while the bulk signal still resembles InGaAs. This suggests the formation of NiAs at the Ni-InGaAs interface, in agreement with the HAXPES results.

The As $3d_{5/2}$ peak can also be used to determine the location of the As-Ni reacted phase with respect to the InGaAs substrate. As such it was measured at higher photon energies, thereby increasing the sampling depth from 6 nm into the InGaAs layer for the As $2p_{3/2}$ peak acquired at 2200 eV photon energy, to 11, 15, and 20 nm for the As $3d_{5/2}$ taken at 2200, 3000 and 4050 eV respectively, as shown in Figure 9 [20]. If the proposed structure of an As-Ni overlayer on the InGaAs substrate is correct, then a more bulk sensitive measurement should be able to detect both As-Ni bonds and As-Ga bonds, attributed to the bulk InGaAs. As can be seen in Figure 9, in the SiN-Ni-InGaAs sample an As-Ga bonding component can be identified at 0.48 eV lower BE than the As-Ni component peak, with the As-Ga peak area increasing with increasing photon energy, as the measurement becomes increasingly bulk sensitive. This confirms the presence of an As-Ni bonding interaction in a layer at the surface of the InGaAs substrate.

In order to determine the relative positions of the NiIn and In-In bonding interactions within the Ni-InGaAs structure, HAXPES spectra were also acquired at 3000 eV photon energy which increases the sampling depth of the In $3d_{5/2}$ from 10 nm at 2200 eV to 13 nm at 3000 eV. From comparison of the normalised spectra following a 300 °C anneal, acquired at the two photon energies, as shown in Figure 10, the change in relative intensity between the In-In and In-Ni can be seen as the photon energy is varied. The results indicate that the In-In is

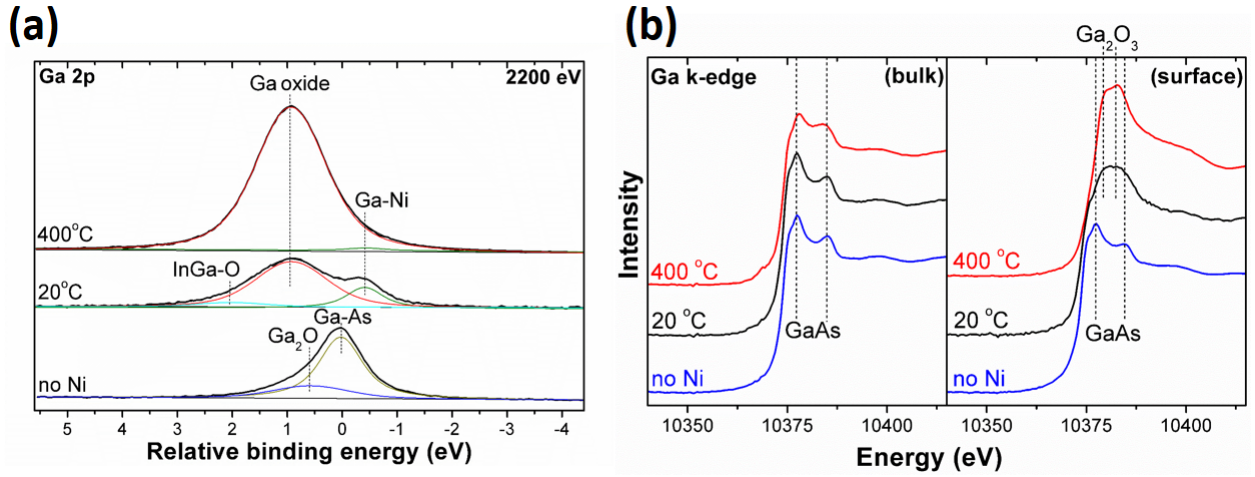


FIG. 6. (a) Normalised and fitted Ga $2p_{3/2}$ HAXPES spectra, and (b) Ga K-edge XAS spectra, for a SiN-InGaAs sample and SiN-Ni-InGaAs samples as-deposited (20 °C), and after a 400 °C anneal. The HAXPES spectra are plotted relative to the binding energy of the substrate Ga-As peak.

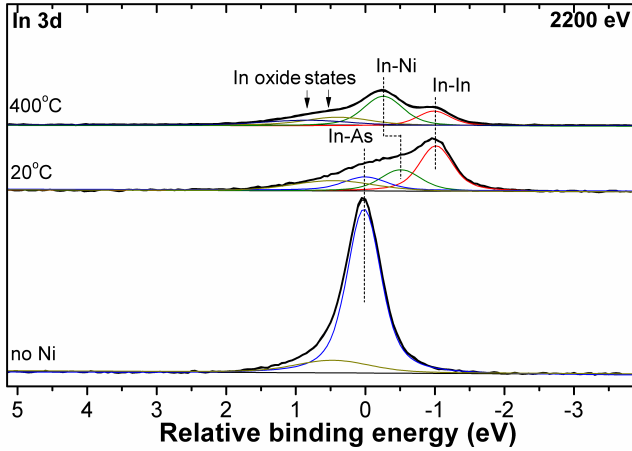


FIG. 7. Normalised and fitted In $3d_{5/2}$ spectra for sample with (20 °C) and without Ni, and after 400 °C anneal. The spectra are plotted relative to the binding energy of the substrate In-As peak.

located below the In-Ni, as in the more bulk sensitive (3000 eV) measurement the In-In intensity increases relative to the In-Ni. A similar comparison for the Ga $2p_{3/2}$ spectra of the as-deposited SiN-Ni-InGaAs sample, where the sampling depth is increased from 7 nm at 2200 eV to 11 nm at 3000 eV, demonstrates the Ga-Ni intensity increasing relative to the Ga oxide in the more bulk sensitive measurement, indicating the Ga-Ni is located below the Ga oxide in the interface structure.

In order to produce an accurate model of the sample structure throughout the anneal study, it is important to understand the location of each chemical species. To this end the photoionisation cross section and inelastic mean free path (IMFP) normalised HAXPES peak areas, referenced with respect to the 3 nm SiN capping layer, are

plotted as a function of anneal temperature for each sample in Figure 11. The error bars in Figure 11 are taken from the discrepancy between the experimental data and the theoretical fit acquired using the XPS fitting software. The steady decrease in the Ni $2p_{3/2}$ signal intensity as a function of anneal temperature is consistent with both the diffusion of Ni into the InGaAs layer as well as the growth of an overlayer of Ga₂O₃. Conversely, the increase of the Ga signal over the course of the anneal study agrees with the continual up-diffusion of Ga through the Ni layer, forming a Ga₂O₃ overlayer between the SiN and Ni layers. The Ga area begins to decrease after the 500 °C anneal, which can be explained by the agglomeration of the Ni-InGaAs layer at this temperature, resulting in the unreacted substrate InGaAs moving toward the sample surface around the agglomerated region. A steady decrease in both the In $3d_{5/2}$ and As $2p_{3/2}$ signals up to 400 °C agrees with both of these elements out-diffusing less than the Ga and remaining closer to the InGaAs surface. The increases seen in both peaks between 450 and 500 °C are due to the Ni-InGaAs agglomeration at these temperatures which significantly disrupts the overall film structure. The segregation of Ga to the top of the interacted layer has also been seen in studies of Ni-GaAs, where Ni₂GaAs is detected upon deposition and this segregates into NiGa near the sample surface, and NiAs near the GaAs substrate, following thermal anneal [13, 43]. The much lower formation energy of Ga₂O₃ as opposed to Ni oxides is consistent with the conversion of the surface localised NiGa into a Ga₂O₃ surface layer [41].

Combining the results from both XAS and HAXPES measurements, a model of the Ni-InGaAs system over the course of the anneal study can be produced. All of the chemical interactions observed appear to initiate upon Ni deposition, contrary to previous results [8], and only the volume of the reacted layers changes as the anneal

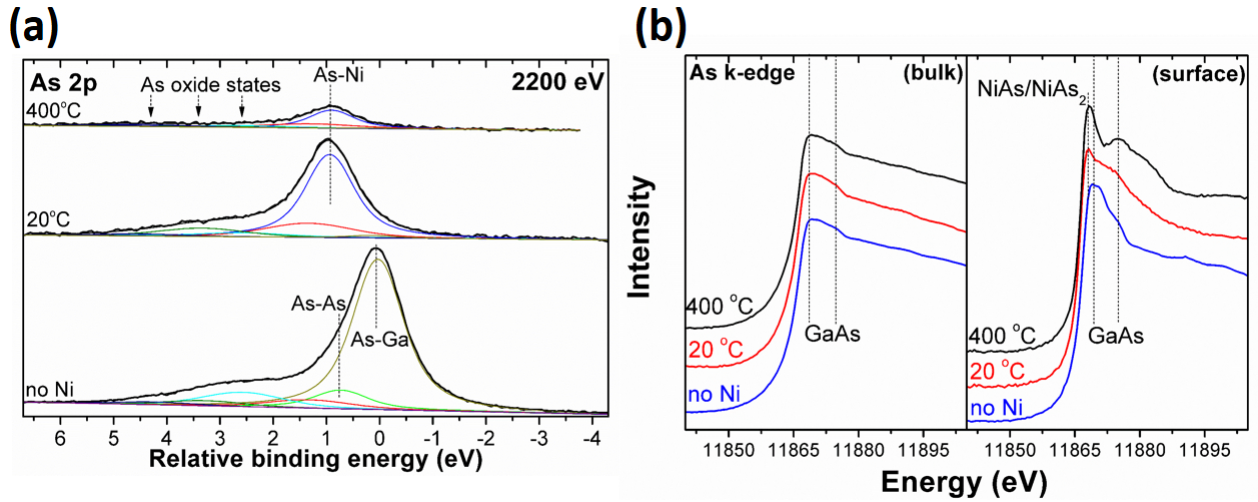


FIG. 8. (a) Normalised and fitted As $2p_{3/2}$ HAXPES spectra for a SiN-InGaAs sample and SiN-Ni-InGaAs samples as-deposited (20 °C) and after a 400 °C anneal (b) As K-edge XAS spectra, for a SiN-InGaAs sample and SiN-Ni-InGaAs samples as-deposited (20 °C), after a 400 °C anneal. The HAXPES spectra are plotted relative to the binding energy of the substrate As-Ga peak.

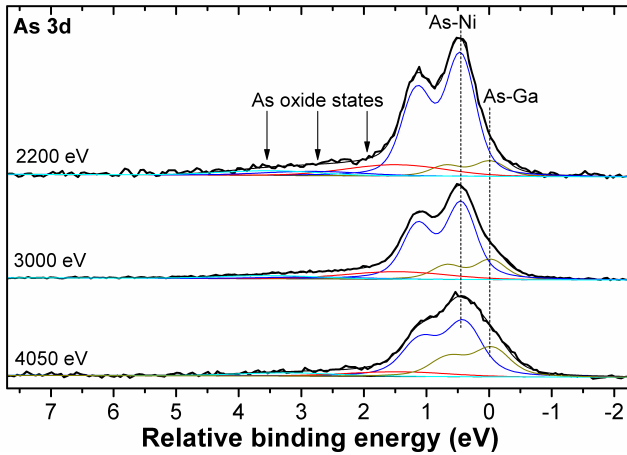


FIG. 9. Normalised and fitted As $3d_{5/2}$ spectra for an as-deposited SiN-Ni-InGaAs sample taken at 2200, 3000, and 4050 eV photon energy. The spectra are plotted relative to the binding energy of the substrate As-Ga peak.

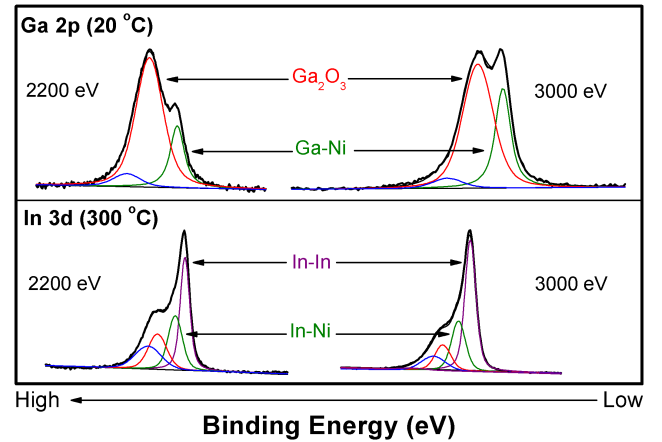


FIG. 10. Normalised and fitted Ga $2p_{3/2}$ spectra for an as-deposited (20 °C) SiN-Ni-InGaAs sample and In $3d_{5/2}$ spectra for a SiN-Ni-InGaAs sample after a 300 °C anneal, acquired at 2200 and 3000 eV photon energy.

temperature increases as Ni continues to diffuse into the InGaAs layer. This expansion of the reacted Ni-InGaAs layer results in the trend of decreasing sheet resistance as a function of temperature seen in Figure 1. The HAXPES and XAS experimental data can be used to construct a schematic model of the sample structure prior to Ni deposition, upon Ni deposition, and after a 400 °C anneal, as shown in Figure 12. The diverse range of the chemical species formed coupled with their physical location in relation to the original Ni-InGaAs interface makes this a challenging experimental study which necessitated the enhanced sampling depth of HAXPES and the definitive chemical species identification capabilities of XAS. Previous studies have described a very abrupt

Ni-InGaAs/InGaAs interface, and constant composition throughout the Ni-InGaAs layer [6–8]. The results in this study are contrary to these findings, as significant diffusion of certain species throughout the anneal study indicate a graded layered structure within the reacted region. These previous studies used secondary ion mass spectroscopy (SIMS) to characterise the diffusion profile of each element as well as the abruptness of the interface. While SIMS is a powerful method in determining the diffusion profile for a given element, the measurement in itself can cause intermixing and it does not provide chemical speciation. The key point in this study is that the combination of HAXPES measurements to identify reactions between Ni and InGaAs, and the dif-

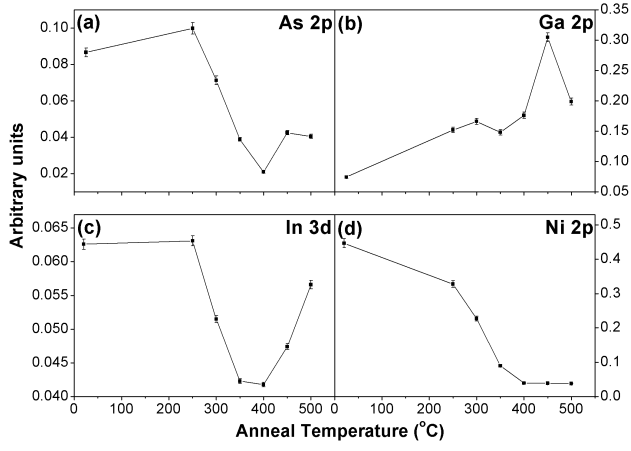


FIG. 11. Plots of the normalised HAXPES peak areas as a function of temperature, of (a) As $2p_{3/2}$, (b) Ga $2p_{3/2}$, (c) In $3d_{5/2}$, and (d) Ni $2p_{3/2}$ peaks. All areas have been normalised by photo-ionisation cross-section, and inelastic mean free path.

fusion profile of the elements throughout the Ni-InGaAs layer, and XAS measurements to provide chemical speciation allows the chemical compositional structure of this complex material system to be investigated. As minimising the source/drain contact resistance is a key requirement for low power devices, the ability to correlate the chemical and electrical measurements facilitates the development of a more comprehensive understanding of the relationship between the chemical compositional profile and the conduction properties.

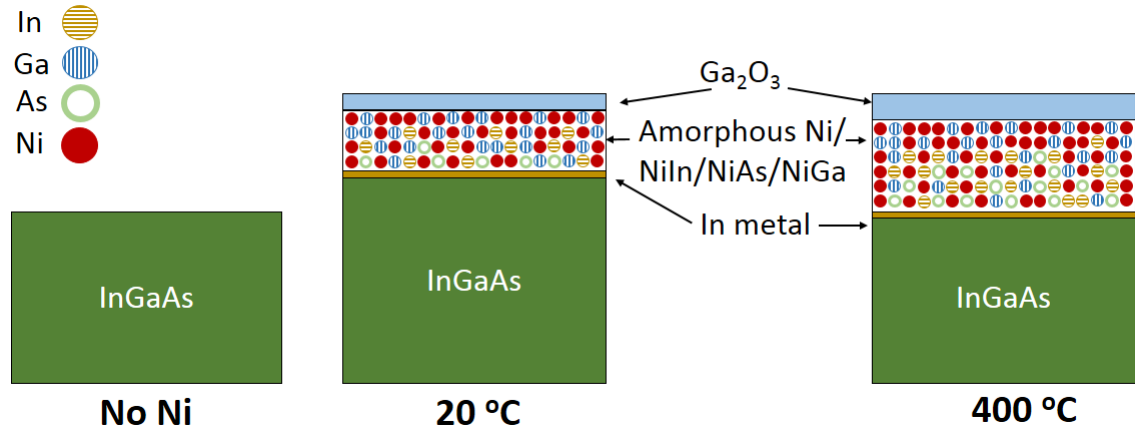


FIG. 12. Schematic diagram showing the deduced Ni-InGaAs sample structure and composition before and after (20 °C) Ni deposition and following 400 °C anneal.

IV. CONCLUSIONS

The change in chemical composition, physical structure and the accompanying change in resistivity of a Ni-InGaAs interface was studied as a function of post deposition anneal temperature. It was found that while the resistivity steadily decreases as the anneal temperature increases for thick films, thinner films show a reversal of this trend at 450 °C due to the agglomeration/phase separation of the Ni-InGaAs film. The decrease in sheet resistance with anneal temperature is due to the increase in thickness of the Ni-InGaAs interaction layer containing Ni-In, Ni-As and Ni-Ga bonds. The analysis of both the chemical and structural composition of Ni-InGaAs contacts has been shown to significantly benefit from the use of two complementary measurement techniques. While XAS can readily identify the chemical species present, HAXPES is required to determine the relative concentrations and diffusion trends throughout the annealing study. The combination of XAS and HAXPES analysis is necessary to fully describe the chemical composition and

structure of the Ni-InGaAs layer. The Ni-InGaAs model derived from the experimental results reveals a highly reactive and inter-diffused interface with substantive Ga out-diffusion and the formation of Ni-In and Ni-As alloy phases closer to the Ni-InGaAs interface. These studies provide a detailed understanding of this material system and have potential application for fabrication strategies for S/D contacts in future InGaAs MOSFETs.

ACKNOWLEDGMENTS

The authors from Dublin City University acknowledge the financial support of SFI under Grant Number: SFI/09/IN.1/I2633. Access to the X24A HAXPES beamline, and the X23A2 XAS beamline at Brookhaven National Laboratory was obtained through a General User Proposal. Use of the National Synchrotron Light Source, Brookhaven National Laboratory, was supported by the U.S. Department of Energy, Office of Science, Office of Basic Energy Sciences, under Contract No. DE-AC02-98CH10886.

-
- [1] Patrick S. Lysaght, Joel Barnett, Gennadi I. Bersuker, Joseph C. Woicik, Daniel A. Fischer, Brendan Foran, Hsing-Huang Tseng, and Raj Jammy. Chemical analysis of HfO₂/Si (100) film systems exposed to NH₃ thermal processing. *Journal of Applied Physics*, 101(2):024105–024105–9, January 2007.
 - [2] Y. T. Chen, J. Huang, J. Price, P. Lysaght, D. Veksler, C. Weiland, J.C. Woicik, G. Bersuker, R. Hill, J. Oh, P.D. Kirsch, R. Jammy, and J.C. Lee. III-V gate stack interface improvement to enable high mobility 11nm node CMOS. In *2012 International Symposium on VLSI Technology, Systems, and Applications (VLSI-TSA)*, pages 1–2, 2012.
 - [3] J. Huang, N. Goel, P. Lysaght, D. Veksler, P. Nagaiah, S. Oktyabrysky, J. Price, H. Zhao, Y.T. Chen, J.C. Lee, J.C. Woicik, P. Majhi, P.D. Kirsch, and R. Jammy. Detailed high- κ /In_{0.53}Ga_{0.47}As interface understanding to enable improved In_{0.53}Ga_{0.47}As gate stack quality. In *2011 International Symposium on VLSI Technology, Systems and Applications (VLSI-TSA)*, pages 1–2, 2011.
 - [4] Han Zhao, Jeff Huang, Yen-Ting Chen, Jung Hwan Yum, Yanzhen Wang, Fei Zhou, Fei Xue, and Jack C. Lee. Effects of gate-first and gate-last process on interface quality of In_{0.53}Ga_{0.47}As metal-oxide-semiconductor capacitors using atomic-layer-deposited Al₂O₃ and HfO₂ oxides. *Applied Physics Letters*, 95(25):253501–253501–3, December 2009.
 - [5] Jonathon B. Clemens, Sarah R. Bishop, Joon Sung Lee, Andrew C. Kummel, and Ravi Droopad. Initiation of a passivated interface between hafnium oxide and In(Ga)As(001)(42). *The Journal of Chemical Physics*, 132(24):244701–244701–8, June 2010.
 - [6] Xingui Zhang, Huaxin Guo, Xiao Gong, Qian Zhou, You-Ru Lin, Hau-Yu Lin, Chih-Hsin Ko, Clement H. Wann, and Yee-Chia Yeo. In_{0.53}Ga_{0.47}As channel n-MOSFET with self-aligned NiInGaAs source and drain. *Electrochemical and Solid-State Letters*, 14(2):H60–H62, February 2011.
 - [7] L. Czornomaz, M. El Kazzi, M. Hopstaken, D. Caimi, P. Mchler, C. Rossel, M. Bjoerk, C. Marchiori, H. Siegwart, and J. Fompeyrine. CMOS compatible self-aligned S/D regions for implant-free InGaAs MOSFETs. *Solid-State Electronics*, 74:71–76, August 2012.
 - [8] Ivana, Yong Lim Foo, Xingui Zhang, Qian Zhou, Jisheng Pan, Eugene Kong, Man Hon Samuel Owen, and Yee-Chia Yeo. Crystal structure and epitaxial relationship of Ni₄InGaAs₂ films formed on InGaAs by annealing. *Journal of Vacuum Science & Technology B: Microelectronics and Nanometer Structures*, 31(1):012202, 2013.
 - [9] Xingui Zhang, Ivana, Hua Xin Guo, Xiao Gong, Qian Zhou, and Yee-Chia Yeo. A self-aligned Ni-InGaAs contact technology for InGaAs channel n-MOSFETs. *Journal of The Electrochemical Society*, 159(5):H511–H515, January 2012.
 - [10] L. J. Brillson, C. F. Brucker, A. D. Katnani, N. G. Stoffel, and G. Margaritondo. Atomic and electronic structure of InPmetal interfaces: A prototypical IIIV compound semiconductor. *Journal of Vacuum Science and Technology*, 19(3):661–666, 1981.
 - [11] T. Kendelewicz, M. D. Williams, W. G. Petro, I. Lindau, and W. E. Spicer. Interfacial chemistry and schottky-barrier formation of the Ni/InP(110) and Ni/GaAs(110) interfaces. *Physical Review B*, 32(6):3758–3765, 1985.
 - [12] R.H. Williams, A. McKinley, G.J. Hughes, V. Montgomery, and I. T. McGovern. Metal-GaSe and metal-InP interfaces: Schottky barrier formation and interfacial reactions. *Journal of Vacuum Science and Technology*, 21(2):594–598, 1982.
 - [13] M.D. Williams, W.G. Petro, T. Kendelewicz, S.H. Pan, I. Lindau, and W.E. Spicer. An exploratory study of the

- reactive Ni-GaAs (110) interface. *Solid State Communications*, 51(10):819–822, September 1984.
- [14] R.T.P. Lee, R.J.W. Hill, W.-Y. Loh, R.-H. Baek, S. Deora, K. Matthews, C. Huffman, K. Majumdar, T. Michaelak, C. Borst, P.Y. Hung, C.-H. Chen, J.-H. Yum, T.-W. Kim, C.Y. Kang, Wei-E. Wang, D.-H. Kim, C. Hobbs, and P.D. Kirsch. VLSI processed InGaAs on Si MOS-FETs with thermally stable, self-aligned Ni-InGaAs contacts achieving: Enhanced drive current and pathway towards a unified contact module. In *Electron Devices Meeting (IEDM), 2013 IEEE International*, pages 2.6.1–2.6.4, December 2013.
 - [15] S. Hofmann. Quantitative depth profiling in surface analysis: A review. *Surface and Interface Analysis*, 2(4):148–160, August 1980.
 - [16] Keisuke Kobayashi. High-resolution hard x-ray photoelectron spectroscopy: Application of valence band and core-level spectroscopy to materials science. *Nuclear Instruments and Methods in Physics Research Section A: Accelerators, Spectrometers, Detectors and Associated Equipment*, 547(1):98–112, July 2005.
 - [17] K. Kakushima, K. Okamoto, K. Tachii, J. Song, S. Sato, T. Kawanago, K. Tsutsui, N. Sugii, P. Ahmet, T. Hattori, and H. Iwai. Observation of band bending of metal/high- κ Si capacitor with high energy x-ray photoemission spectroscopy and its application to interface dipole measurement. *Journal of Applied Physics*, 104(10):104908–104908–5, November 2008.
 - [18] Dale E. Sayers, Edward A. Stern, and Farrel W. Lytle. New technique for investigating noncrystalline structures: Fourier analysis of the extended x-ray absorption fine structure. *Physical Review Letters*, 27(18):1204–1207, November 1971.
 - [19] C. Weiland, P. Lysaght, J. Price, J. Huang, and J. C. Woicik. Hard x-ray photoelectron spectroscopy study of as and ga out-diffusion in $\text{In}_{0.53}\text{Ga}_{0.47}\text{As}/\text{Al}_2\text{O}_3$ film systems. *Applied Physics Letters*, 101(6):061602, August 2012.
 - [20] S. Tanuma, C. J. Powell, and D. R. Penn. Calculations of electron inelastic mean free paths. IX. data for 41 elemental solids over the 50 eV to 30 keV range. *Surface and Interface Analysis*, 43(3):689–713, 2011.
 - [21] Jill Chastain and John F Moulder. *Handbook of X-ray photoelectron spectroscopy : a reference book of standard spectra for identification and interpretation of XPS data*. Physical Electronics, Eden Prairie, Minn., 1995.
 - [22] D. A. Shirley. High-resolution x-ray photoemission spectrum of the valence bands of gold. *Physical Review B*, 5(12):4709–4714, June 1972.
 - [23] Patrick S. Lysaght, Joseph C. Woicik, Jeff Huang, Jungwoo Oh, Byoung-Gi Min, and Paul D. Kirsch. Process driven oxygen redistribution and control in $\text{Si}_{0.7}\text{Ge}_{0.3}/\text{HfO}_2/\text{TaN}$ gate stack film systems. *Journal of Applied Physics*, 110(8):084107, October 2011.
 - [24] Barry Brennan. *Surface and interface characterisation of high- κ dielectric materials on silicon and III-V semiconductor substrates*. doctoral, Dublin City University. School of Physical Sciences, March 2010.
 - [25] G. Dalba, D. Diop, P. Fornasini, A. Kuzmin, and F. Rocca. EXAFS and XANES study of GaAs on Ga and As K-edges. *Journal of Physics: Condensed Matter*, 5(11):1643, March 1993.
 - [26] M. G. Proietti, S. Turchini, J. Garcia, G. Lamble, F. Martelli, and T. Prosperi. Glancing-angle extended x-ray absorption fine structure study of strained InGaAs/GaAs heterostructures. *Journal of Applied Physics*, 78(11):6574–6583, 1995.
 - [27] P. Pianetta, I. Lindau, C. M. Garner, and W. E. Spicer. Oxidation properties of GaAs (110) surfaces. *Physical Review Letters*, 37(17):1166–1169, October 1976.
 - [28] S. I. Raider, R. Flitsch, J. A. Aboaf, and W. A. Pliskin. Surface oxidation of silicon nitride films. *Journal of The Electrochemical Society*, 123(4):560–565, April 1976.
 - [29] Andrew P. Grosvenor, Mark C. Biesinger, Roger St.C. Smart, and N. Stewart McIntyre. New interpretations of XPS spectra of nickel metal and oxides. *Surface Science*, 600(9):1771–1779, May 2006.
 - [30] Li-Shing Hsu, Y.-K. Wang, and G. Y. Guo. Experimental and theoretical study of the electronic structures of Ni_3Al , Ni_3Ga , Ni_3In , and NiGa . *Journal of Applied Physics*, 92(3):1419–1424, August 2002.
 - [31] Anna Puig-Molina, Lars Pleth Nielsen, Alfons M. Molenbroek, and Konrad Herbst. In situ EXAFS study on the chemical state of arsenic deposited on a $\text{NiMoP}/\text{Al}_2\text{O}_3$ hydrotreating catalyst. *Catalysis Letters*, 92(1-2):29–34, January 2004.
 - [32] C. L. Hinkle, M. Milojevic, B. Brennan, A. M. Sonnet, F. S. Aguirre-Tostado, G. J. Hughes, E. M. Vogel, and R. M. Wallace. Detection of Ga suboxides and their impact on III-V passivation and fermi-level pinning. *Applied Physics Letters*, 94(16):162101, April 2009.
 - [33] David R. Lide. *Handbook of Chemistry and Physics: 2004-2005*. CRC Press LLC, June 2004.
 - [34] L. J. Brillson, C. F. Brucker, N. G. Stoffel, A. D. Katnani, and G. Margaritondo. Abruptness of semiconductor-metal interfaces. *Physical Review Letters*, 46(13):838–841, March 1981.
 - [35] S. Huang, B. Shen, F. Lin, N. Ma, F. J. Xu, Z. L. Miao, J. Song, L. Lu, F. Liu, Y. Wang, Z. X. Qin, Z. J. Yang, and G. Y. Zhang. Ni diffusion and its influence on electrical properties of $\text{Al}_x\text{Ga}_{1-x}\text{N}/\text{GaN}$ heterostructures. *Applied Physics Letters*, 93(17):172102–172102–3, October 2008.
 - [36] Emiel J. M. Hensen, Mayela Garca-Sánchez, Neelesh Rane, Pieter C. M. M. Magusin, Pang-Hung Liu, Kuei-Jung Chao, and R. A. van Santen. In situ Ga K-edge XANES study of the activation of Ga/ZSM-5 prepared by chemical vapor deposition of trimethylgallium. *Catalysis Letters*, 101(1-2):79–85, May 2005.
 - [37] Ken-ichi Shimizu, Atsushi Satsuma, and Tadashi Hattori. Metal oxide catalysts for selective reduction of NO_x by hydrocarbons: Toward molecular basis for catalyst design. *Catalysis Surveys from Japan*, 4(2):115–123, July 2001.
 - [38] Seong-Kyun Cheong, Bruce A. Bunker, D. C. Hall, G. L. Snider, and P. J. Barrios. XAFS and x-ray reflectivity study of IIIV compound native oxide/GaAs interfaces. *Journal of Synchrotron Radiation*, 8(2):824–826, March 2001.
 - [39] D. J. Fu, Y. H. Kwon, T. W. Kang, C. J. Park, K. H. Baek, H. Y. Cho, D. H. Shin, C. H. Lee, and K. S. Chung. GaN metaloxidesemiconductor structures using Ga-oxide dielectrics formed by photoelectrochemical oxidation. *Applied Physics Letters*, 80(3):446–448, January 2002.
 - [40] F.L. Riley. Silicon nitride and related materials. *Journal of the American Ceramic Society*, 83(2):245–265, 2000.

- [41] Donald D. Wagman, William H. Evans, Vivian B. Parker, Richard H. Schumm, Iva Halow, Sylvia M. Bailey, Kenneth L. Churney, and Ralph L. Nuttall. *The NBS Tables of Chemical Thermodynamic Properties*, volume 11. National Bureau of Standards.
- [42] Shunsuke Sakai, Akira Yoshiasa, Hiroshi Arima, Maki Okube, Chiya Numako, and Tsutomu Sato. XAFS study of As in K-T boundary clays. *AIP Conference Proceedings*, 882(1):274–276, February 2007.
- [43] Masaki Ogawa. Alloying reaction in thin nickel films deposited on GaAs. *Thin Solid Films*, 70(1):181–189, July 1980.